Revisiting ISR Spectra Modeling: Higher-Order Stochastic Approach and Surrogate Models

ITIT-23

BRIAN LA ROSA[1], ENRIQUE ROJAS [1], MARCO MILLA[2]

[1]Cornell University , [2]Pontifical Catholic University of Peru

bl639@cornell.edu

INTRODUCTION

The most complete analytical model for F-Region plasma particle dynamics, which includes the **Coulomb collision effect,** was described by Milla & Kudeki (2011) . *The* β and *D* are known as Spitzer coefficients which have large values for electron dynamic. *U* is a Gaussian white noise vector. This approach force the use of small time-step discretization (*dt*<<1) for a Euler-Maruyama algorithm, generating a high computational execution time. The stiffness behavior of this model require a better computational treatment to increase efficiency. A wide exploration on SDE numerical solvers have been covered and numerical benchmarks have been performed.

$$\frac{d\vec{v}}{dt} = \underbrace{-\beta(v)\vec{v}(t)}_{\text{drift}} + \underbrace{\frac{q}{m}\vec{v}(t)\times\vec{B}}_{\text{gyro-term}} + \underbrace{\tilde{D}(v,t)\vec{U}}_{\text{diffusion}}$$

SDE NUMERICAL SOLVERS

Higher-order algorithms based on more complex expansions avoids the use of small time-step discretization, however, more terms are needed to be calculated on each iteration to maintain precision and stability.

$$dX_t = \left(\frac{1}{2}X_t + \sqrt{X_t^2+1}\right)dt + \sqrt{X_t^2+1}\,dW_t$$

A weak convergence test is presented in Figure II, solving the 1D system with analytical solution shown in Debrabant & Robler (2010). This test establish the relationship between precision and computational discretization for solvers listed in table I:

Algorithm	Description	Features
EM	Euler-Maruyama	Explicit, Weak order 1
RDI1WM	Stochastic Runge-Kutta based algorithm	Explicit, Weak order 1
RDI4WM	Stochastic Runge-Kutta based algorithm	Explicit, Weak order 2
RI5	Stochastic Runge-Kutta based algorithm	Explicit, Weak order 2
DRI1	Approximated EM (Drift Condition)	Explicit, Weak order 1

Table I: *List of Stochastic Solvers*

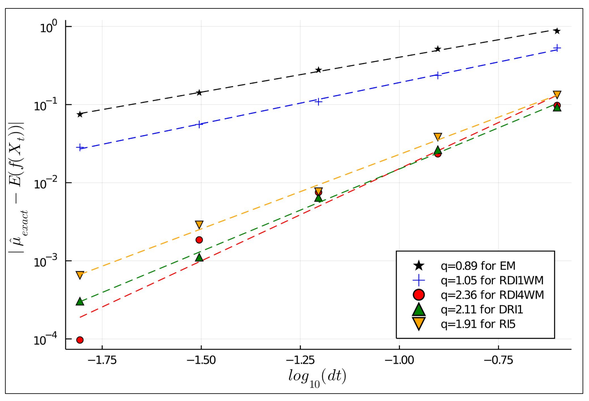

Figure II: *Weak order of convergence (q) analysis for algorithms Listed in Debrabant & Robler (2010)*

Algorithm	dt (s)	Execution Time (s)	Error
Adaptive EM	dt ~ 1/10β	0.923	~ 10^{-1}
	dt ~ 1/100β	5.96	~ 10^{-2}
RDI4WM	0.315	0.17	~ 10^{-1}
	0.1	0.638	~ 10^{-2}

Table II: *Execution time and computational error are measure for Adaptive Euler-Maruyama and RDI4WM*

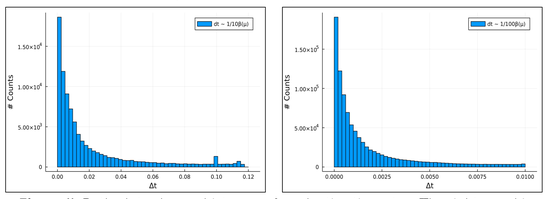

Figure II: *Both plots show a histogram for adaptive time step. The right panel is for the dt ~ 1/10β, and the right panel is for dt ~ 1/100β.*

We identify that *RDI4WM* algorithm has the fewer error measurement from solvers listed in table I. In addition, we are also interested in compare this higher-order algorithm with the adaptive Euler-Maruyama scheme used by Milla & Kudeki to solve their model, explained in Table II. This test also suggests that the RDI4WM algorithm has a greater performance over the adaptive scheme.

SIMULATION

The model is used to simulate the evolution of charged particles on a O^+plasma. The *RDI4WM* algorithm must recover the standard results form particle dynamics as shown in Figure III. This higher-order solver were constructed to handle with stiffness equations like Milla & Kudeki model, which include the Coulomb collision effect. In figure III, variable radius gyromotion behavior is recovered using this new stochastic solver.

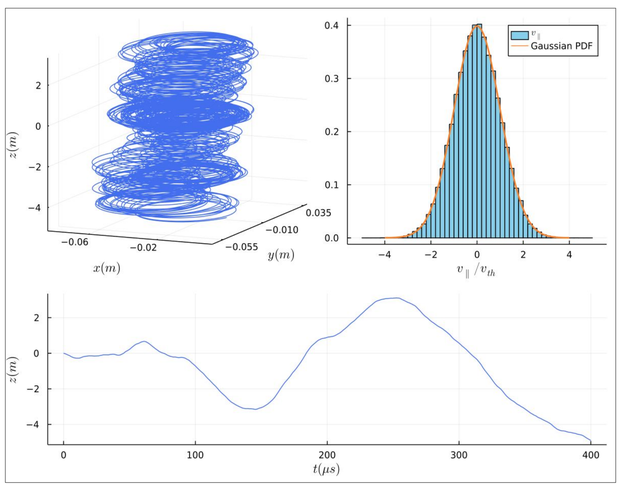

Figure III: *Simulated electron trajectory for an O^+ plasma (T_e= 1e3 K, $N_e = 10^{12}m^{-3}$), with B field aligned to Z-axis using the RDI4WM algorithm. The velocity histogram correspond to the z-direction. Orange line is a analytical Gaussian distribution with mean μ = 0 and variance σ = 1.*

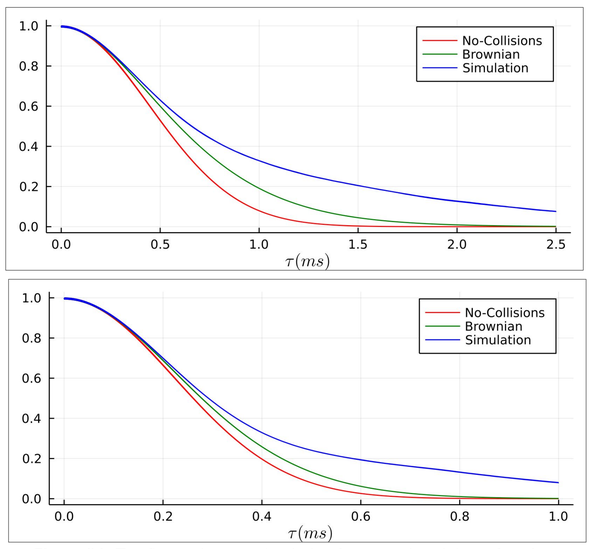

Figure IV : *Top figure shows a simulation for a correlated time of t = 1 ms and an aspect angle of* **α = 1.0°.** *Bottom figure shows a simulation for t = 2.5 ms and aspect angle of* **α = 0.5°**.

However, we must focus on recover the particle displacement, both parallel and perpendicular to the *B* field. To test a good performance of the SDE solvers, a bunch of 5000 trajectories sampled from a normal distribution *~N(0, v_{th})* is used to reproduce the electron Auto Correlation Function (ACF) shown in figure IV.

RESULTS

In this section, we present different parameters scenarios to explore the approximation that electron ACF can be decoupled in a perpendicular and parallel contributions:

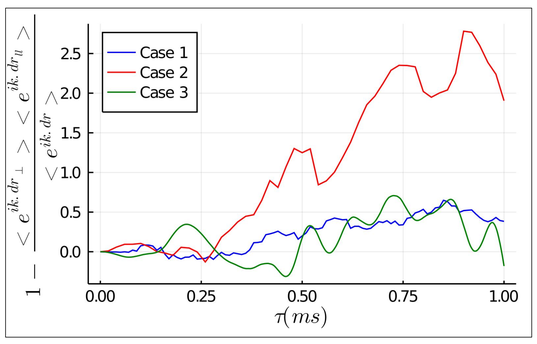

Figure V: *Relative error measurement for electron ACF using*

$$< e^{i\vec{k}\cdot\Delta\vec{r}} > \approx < e^{ik_\perp^{\rightarrow}\cdot\Delta r_\perp^{\rightarrow}} >< e^{ik_\parallel\cdot\Delta r_\parallel} >$$

To explore the sensibility of this assumption we set 3 different scenarios. First, a standard set of parameters (Case 1). Then, a modified temperature, density and magnetic field (Case 2) to test the sensibility of this assumption to physical parameters, and finally, an almost unmagnetized electron dynamics (Case 3).

Case 1	B = 25μT; Te = 1000 K; Ne=1e12
Case 2	B = 12μT; Te = 500 K; Ne=5e12
Case 3	B = 50nT; Te = 1000 K; Ne=1e12

Table III: *List of different physical parameters*

From figure V, it is observed that from the three different scenarios, the relative error of the electron ACF remains under a ~2.5% for the specific parameter combinations shown in table I.

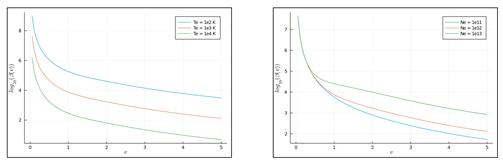

Figure VI: *Drift Spitzer Coefficients dependency from temperature(left), and electron density(right).*

Further, the numerical results from Milla & Kudeki model suggest that the particle displacement distribution along the B field is dominated from a non-Normal distribution. This behaviour was also observed in our simulation using the RDI4WM higher-order algorithm as shown in figure VII. To explore the idea of a non Gaussian distribution Various distributions were tested to fit the statistics of the parallel displacements observed in the simulation for electron particle trajectories The best fit was obtained using a superposition of a Gaussian and a Laplace distributions as shown in Figure VIII: $f(\Delta r_\parallel) = A_G f_G(\sigma) + (1-A_G) f_L(b)$

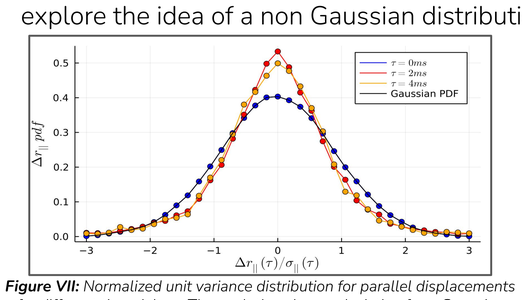

Figure VII: *Normalized unit variance distribution for parallel displacements for different time delays. The evolution show a deviation from Gaussian pdf.*

Because the we assumed that the distributions are symmetric and centered at zero, we can parameterize this model using three parameters:

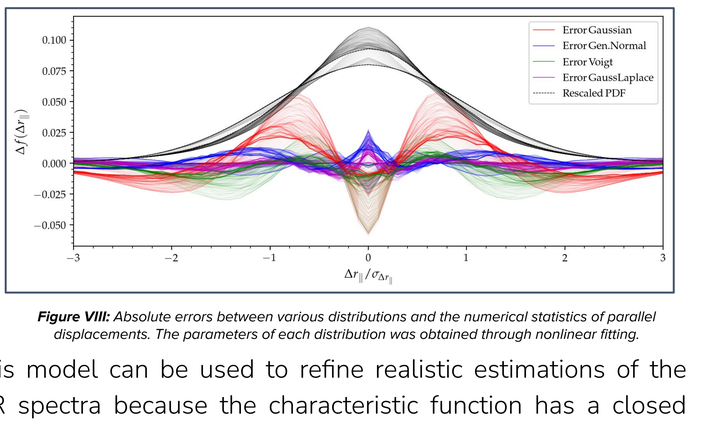

Figure VIII: *Absolute errors between various distributions and the numerical statistics of parallel displacements. The parameters of each distribution was obtained through nonlinear fitting.*

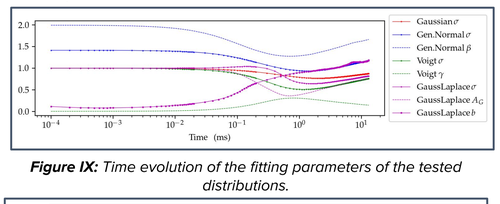

Figure IX: *Time evolution of the fitting parameters of the tested distributions.*

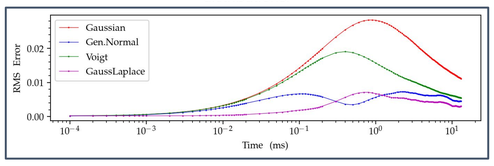

Figure XI*: Time evolution of the RMS error for the tested distributions.*

This model can be used to refine realistic estimations of the ISR spectra because the characteristic function has a closed form. From Figure IX, fitted parameters are calculated among integration time, using the particle parallel displacement distribution generated from the simulation. The RMS error estimation was calculated to validate the proximity of the Gauss Laplace distribution over all time evolution among the other fitted distributions.

CONCLUSIONS

- The *RDI4WM* higher-order numerical algorithm have been used to solved Milla & Kudeki model for the electron particle dynamics, showing a better performance among the others .
- Numerical instability, caused by the stiffness behaviour of the Milla & Kudeki model due to the great values for electron Spitzer coefficients an gyro-term, was controlled with a bigger and fix time-step *dt* = 1e-8. This model simulation can be reproduced faster using the new approach with a reduction on computational time and memory allocation.
- Due to the parallel displacement deviation shown in the Milla & Kudeki model, a statistical analysis was done to determine if these distributions can be fitted to a known distribution . Further analysis is required to establish a better simulation agreement.

ACKNOWLEDGEMENTS

- The authors thank to the CEDAR Workshop committee for their financial support to attend and present this poster.
- We also thanks to the Computational Sciences Department of the Technological University of Peru (UTEC) for the use the Khipu Cluster.

REFERENCES

[1] Kudeki, E. & Milla, M.A. (2011). IEEE Transactions on Geoscience and Remote. Incoherent scatter spectral theories-Part II: A general result for small magnetic asSensing, vol 49, pp 315-328. doi: 10.1109/TGRS.2010.2057252
[2] Debrabant &Robler A. (2010)). Mathematics and Computing in simulations. Classification of Stochastic Runge–Kutta Methods for the Weak Approximation of Stochastic Differential Equations. vol 04, pp 408-420, doi: 10.1016/j.matcom.2007.04.016
[3] Platen, Eckhard (1999). An introduction to numerical methods for stochastic differential equations. Acta Numerica, vol 8, pp 197-246. doi: 10.1017/S0962492900002920
[4] Rackauckas, Christopher and Nie, Qing (2017). The Journal of Open Research Software. A Performant and Feature-Rich Ecosystem for Solving Differential Equations in Julia Vol 5. doi:10.5334/jors.151